

# Monochromatic coherent transition and diffraction radiation from a relativistic electron bunch train

G. Naumenko,<sup>a,\*</sup> A. Potylitsyn,<sup>a</sup> M. Shevelev,<sup>a</sup> P. Karataev,<sup>b</sup> M. Shipulya<sup>c</sup> and V. Bleko<sup>c</sup>

<sup>a</sup> Tomsk Polytechnic University,  
Tomsk, 634050 Russia

<sup>b</sup> John Adams Institute for Accelerator Science, Royal Holloway University of London,  
Egham Hill, Egham, Surrey TW20 0EX, United Kingdom

<sup>c</sup> RASA Center, Tomsk Polytechnic University,  
Tomsk, 634050 Russia

E-mail: [naumenko@tpu.ru](mailto:naumenko@tpu.ru)

**Abstract:** Electron beams of most accelerators have a bunched structure and are synchronized with the accelerating RF field. Due to modulation of the electron beam with frequency  $\nu_{RF}$  one can expect to observe resonances with frequencies  $\nu_k = k \cdot \nu_{RF}$  in radiation spectrum generated via any spontaneous emission mechanism ( $k$  is an integer and the resonance order). In this paper we present the results of spectral measurements of coherent transition radiation (CTR) generated by an electron bunch train from the Tomsk microtron with  $\nu_{RF} = 2.63$  GHz in the spectral frequency range from 8 to 35 GHz. We also measured the spectrum of coherent diffraction radiation and demonstrated that the observed spectra in both cases consist of monochromatic lines. For spectral measurements the Martin-Puplett interferometer with spectral resolution of 800 MHz (FWMH) was employed. Using a waveguide frequency cut-off we were able to exclude several spectral lines to observe higher resonance orders of up to  $k=7$ .

Keywords: coherent radiation; transition radiation; diffraction radiation; monochromaticity.

---

\* Corresponding author.

---

## Contents

<b>1. Introduction</b>	<b>1</b>
<b>2. Experimental setup</b>	<b>3</b>
<b>3. Measurement results</b>	<b>4</b>
<b>4. Discussion</b>	<b>7</b>

---

## 1. Introduction

Recent years a few THz radiation sources based on linacs producing sub picosecond bunches were constructed and commissioned [1,2,3]. The radiation mechanism used to achieve the goal is transition radiation (TR) [4]. A continuous broadband coherent TR (CTR) spectrum is generated by an electron bunch from a conducting target and emitted into an angular cone of order of  $\theta_x, \theta_y \leq \gamma^{-1}$ , where  $\theta_x$  and  $\theta_y$  are the projection observation angles measured from the direction of mirror reflection and  $\gamma$  is the charged particle Lorenz factor. The CTR wavelength range is determined by the outer target dimensions (low frequency limit) and the electron bunch length  $\sigma_z$  (high frequency limit). Diffraction radiation (DR) appears when electrons move in the vicinity of a target [5]. For relativistic electrons the transverse size of electron Coulomb field is treated as  $\gamma\lambda$ , where  $\lambda$  is the wavelength of the investigated radiation. In the pseudo-photon approximation [6] one can consider the backward diffraction radiation as reflection of relativistic electron field by the target surface.

Another application of the CTR process (as well as the coherent diffraction radiation (CDR)) is the measurement of longitudinal profile of ultra short bunches. As a rule one has to measure the CTR / CDR spectrum in order to reconstruct the bunch profile using, for instance, inverse Fourier transform [7]. To determine the bunch length it is necessary to measure the high-frequency range of the CTR spectrum with high accuracy. A train of electron bunches (or a modulated electron beam) can generate quasi-monochromatic radiation. The resulting spectrum consists of a set of the spectral lines (harmonics of the bunching frequency). This is not a trivial task to decode information about the bunch length from such a non-uniform spectrum.

The CTR process generated by an electron beam consisting of a periodic train of bunches was also studied in [3,7,8]. In [9,10,11] the authors investigated this effect for the coherent synchrotron radiation mechanism, in [12] – for the coherent Smith-Purcell radiation. In all cases the spectrum contained monochromatic lines. The origin of those lines comes from constructive interference of radiation generated by successive bunches. This effect was called as the frequency-locked radiation [7]. The authors of [11] have used the term “superradiant radiation” because of the quadratic dependence of the spectral line intensity on the number of bunches.

Despite of the fact that the distance,  $\Lambda$ , between bunches is much larger than the bunch length,  $\sigma_z$ , the CTR spectrum contains monochromatic lines corresponding to high order

resonances [3,13]. Nowadays, the technology of laser photocathode RF guns allows us to obtain a train of femtosecond electron bunches with submillimeter spacing (see, for instance, [14]). A similar train of bunches can also be produced converting the transversely modulated bunch in high dispersion region of accelerator into a temporally separated set of micro bunches by a set of dipole magnets [15]. In [16] the authors measured the CTR spectrum from six ultra-short electron bunches ( $\sigma_z \leq 20 \mu\text{m}$ ) separated by  $\Lambda = 700 \mu\text{m}$  and showed that the spectrum contains the fundamental harmonic with the frequency  $\nu_1 = c/\Lambda = 0.43 \text{ THz}$  ( $c$  is the speed of light) and the second harmonic  $\nu_2 = 2c/\Lambda = 0.86 \text{ THz}$ . However, the mechanism of formation of such highly monochromatic beams, limitations in wavelength and train length are not very well studied and understood yet.

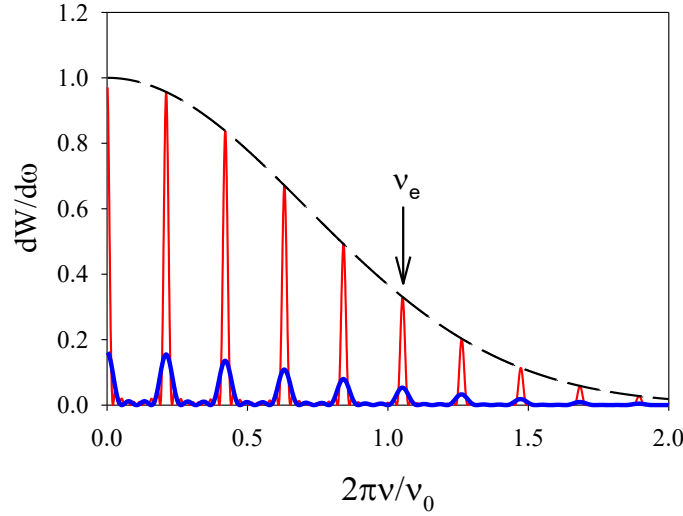


**Figure 1.** Normalized CTR spectrum from a single bunch (black dashed line), CTR from a train for  $N_b=10$  (red solid line) and for  $N_b=4$  (bold blue line, normalized on the line for  $N_b=10$ )

In the frequency range around  $\gamma c/a \leq \omega \leq \omega_p$  the spectrum of backward transition radiation emitted by a single charged particle in a cone with opening angle of  $\theta_{x,y} \sim \gamma^{-1}$  can be considered as a constant ( $dW_{\text{inc}}/d\omega = \text{const}$ ) with high enough accuracy. Here  $a$  is the transverse size of the target and  $\omega_p$  is the plasmon frequency of the target matter [17,18]. The CTR spectrum generated by an electron bunch with the length  $\sigma_z$  (rms) can be presented as

$$\frac{dW_{\text{coh}}}{d\omega} = N_e^2 F_e(\omega) \frac{dW_{\text{inc}}}{d\omega}, \quad (1)$$

where  $F_e(\omega) = \exp(-\omega^2 \sigma_z^2 / c^2) = \exp(-(2\pi\nu/\nu_0)^2)$  is the form factor for the Gaussian distribution, describing the longitudinal bunch profile,  $\nu_0 = c/\sigma_z$  and  $N_e$  is the number of electrons in the bunch. Figure 1 (dashed line) shows the typical normalized CTR spectrum obtained neglecting the effect of the outer target dimensions on low-frequency part. The spectrum of coherent radiation from a train of  $N_b$  bunches should be multiplied by the train form factor [3]

$$G_{\text{train}}(\omega) = \left[ \frac{\sin(N_b \omega \Lambda / 2c)}{\sin(\omega \Lambda / 2c)} \right]^2. \quad (2)$$

Therefore the resultant spectrum is:

$$\frac{dW_{\text{train}}}{d\omega} = N_e^2 F_e(\omega) G_{\text{train}}(\omega) \frac{dW_{\text{inc}}}{d\omega} \quad (3)$$

Since the maximal value of the form factor (2) is equal to  $N_b^2$ , the maxima in the spectrum are determined by the quantity  $N_b^2 N_e^2$ .

Figure 1 illustrates the normalized CTR spectrum from a single bunch (black dashed line), CTR from a train for  $N_b=10$  (red solid line), and  $N_b=4$  (bold blue line, normalized on the line for  $N_b=10$ ) for  $\Lambda = 30 \sigma_z$ . The relative bandwidth of  $k$ -th line is defined by the number of bunches as  $(\Delta\nu_k / \nu_k \sim 1/N_b)$ . The frequency,  $\nu_e$ , corresponding to the  $1/e$  fraction of the CTR maximum level allows us to determine the frequency  $\nu_0 = 2\pi\nu_e$  and to evaluate  $\sigma_z = c/2\pi\nu_e$ . The frequency interval between two successive spectral peaks depends on the distance between bunches as  $\Delta\nu = c/\Lambda$  or, for conventional accelerators,  $\Delta\nu = \nu_{RF}$ . The spectral distribution consists of many spectral lines with frequencies  $k \cdot \Delta\nu$ ,  $k \gg 1$ . Intensity and width of monochromatic lines depend on the effective number of bunches producing radiation synchronously. Nevertheless, figure 1 shows that the envelope of the bunch form factor is independent of the number of bunches in a train.

In this paper we have measured CTR and CDR spectra produced by a multi-bunched electron beam from the 6-MeV electron microtron. We have demonstrated that using cut-off wave guide we can select a certain part of the spectrum and reinforce some lines versus the others.

## 2. Experimental setup

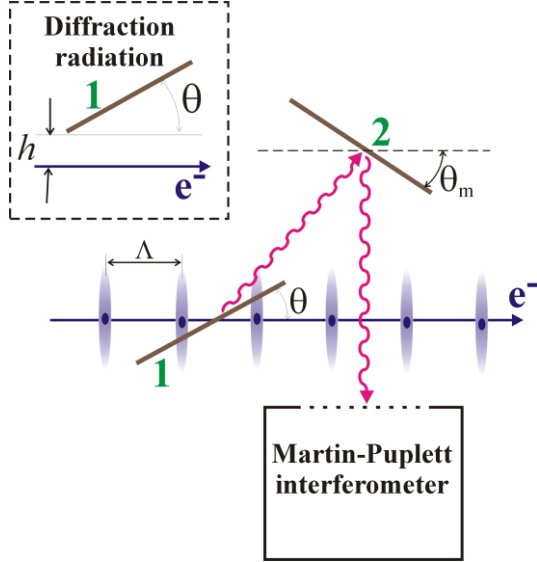
The experiment was carried out using the electron beam extracted from microtron of the Tomsk Polytechnic University. The parameters are listed in Table 1.

Table 1. Electron beam parameters

Electron energy	$E_e=6.1 \text{ MeV } (\gamma = 12)$
Macro-pulse (train) duration	$4 \mu\text{s}$
Bunch length	$\sigma_z = 3 \pm 1 \text{ mm}$
Bunch population	$N_e=10^8$
Bunches in train	$N_b=10^4$
Distance between bunches	$\Lambda = 114 \text{ mm } (\nu_{RF} = 2.63 \text{ GHz})$
Transverse beam size	$4 \times 2 \text{ mm}$

The radiation with frequency of  $\nu \leq 33.3 \text{ GHz}$  is emitted coherently [20] due to the fact that its wavelength is longer than the bunch length. The experimental layout is shown in figure 2. The bunched electron beam generates CTR from the conductive target 1. The radiation is reflected from mirror 2 placed at an angle  $\theta_m = 45^\circ$  relative to the electron beam trajectory and analyzed using Martin-Puplett interferometer. The CDR geometry is shown in the insertion in figure 2, where  $h$  is the impact parameter, i.e. the minimal distance from the electron beam trajectory to the target. The size of the copper target 1 and the mirror 2 is  $300 \times 200 \text{ mm}$ . The target could be rotated around its vertical axis for radiation orientation dependence measurements (co-called  $\theta$ -scan, where  $\theta$  is the angle between target surface and electron

beam trajectory). The spectral measurements were performed using Martin–Puplett interferometer [21-23] (see figure 3) elaborated for millimeter wavelength range, whose parameters are summarized in Table 2. The frequency resolution  $\Delta\nu_{\text{exp}}$  of the interferometer is defined by the maximal optical path  $\Delta l$  difference achieved by the movable mirror  $M_2$ :  $\Delta\nu_{\text{exp}} \approx c/\Delta l$  and in our case  $\Delta\nu_{\text{exp}} \approx 0.8 \text{ GHz}$  ( $\Delta\nu_{\text{exp}} < \nu_{RF}$ ).



**Figure 2.** Layout of experiment. 1 is the target, 2 is the conductive mirror. Insertion shows the target geometry for the case of CDR measurement

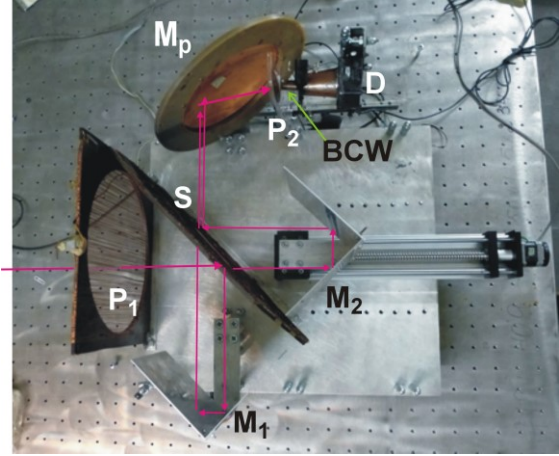


**Figure 3.** The Martin-Puplett interferometer. Definitions:  $P_1$  and  $P_2$  are the polarizers,  $S$  is the polarization splitter,  $M_p$  is the parabolic mirror with focus length of  $f = 95 \text{ mm}$ ,  $M_1$  is the fixed roof mirror,  $M_2$  is the movable roof mirror,  $D$  is the detector,  $BCW$  is the cut-off wave-guide.

**Table 2.** Interferometer parameters and notations

Fixed mirror $M_1$	$170 \times 170 \text{ mm}$
Movable mirror $M_2$	$170 \times 170 \text{ mm}$
Parabolic mirror $M_p$	$\varnothing = 210 \text{ mm}, f = 95 \text{ mm}$
Polarizer $P_1, P_2$	$\varnothing = 230, 70 \text{ mm}$
Splitter $S$	$\varnothing_{pr} = 210 \text{ mm}$
Cut-off wave-guide	$\varnothing = 10, 15, 20 \text{ mm}$
<b>BCW</b>	$\nu > 17.6, 11.8, 8.8 \text{ GHz}$
Detector <b>D</b>	DPMM-01
Path of mirror $M_2$	$\Delta l = 300 \text{ mm}$

To choose the target orientation for spectral measurements we performed the  $\theta$  - scan (see figure 4). The movable mirror of the interferometer was placed in a position where two arms of the interferometer are equal in length.

The detector ( $D$  in figure 3) is the room-temperature detector DPMM-01 based on a broadband antenna with low-threshold high frequency diode [13]. The detector spectral efficiency is  $4 \text{ mm} < \lambda < 50 \text{ mm}$ . However, the high frequency part of the CTR/CDR spectra are limited by the longitudinal electron bunch form-factor determining the radiation coherency ( $\lambda_{\text{min}} > 10 \text{ mm}$ ). The cut-off wave-guide ( $BCW$  in figure 3) was used to cut the noise of the accelerator RF system and select a certain part of the spectrum.

### 3. Measurement results

At the first stage we measured the  $\theta$ -scan of the CTR yield (see figure 4) using the cut-off wave-guide with diameter of  $\varnothing = 20$  mm (cutting out the frequencies  $\nu < 8.8$  GHz). The dependence demonstrates a typical TR behavior with a minimum along the specular reflection direction and two asymmetric maxima because the Lorenz-factor is small and target is tilted with respect to the beam trajectory [24]. Spectral measurements were carried out for the large maximum at the angle  $\theta_1 = 18.5^\circ$ .

The obtained interferogram using the same cut-off wave-guide is presented in insertion in figure 5. To reconstruct the spectrum from the measured interferogram we applied the Fourier transform algorithm from [19]. The interferogram has a periodic macrostructure (amplitude modulation) with the period of  $\Lambda/2$ . A practically ideal coincidence of the modulation period with a half of the distance between bunches suggests that this is the result of interference of radiation from subsequent bunches.

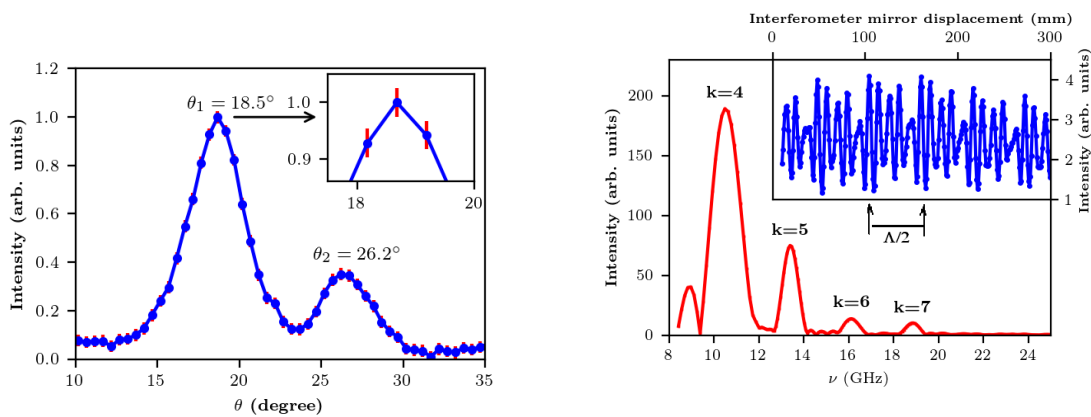


**Figure 4.** CTR orientation dependence ( $\theta$ -scan).

**Figure 5.** Spectrum reconstructed from the observed interferogram shown in insertion.

The positions of measured maxima in figure 5,  $\nu_p$ , are well described by the equation  $\nu_k = k \cdot c / \Lambda$ . The analysis of the maxima is summarized in Table 3. Therefore, we can confidently conclude that we observe the intra-train interference effect in the CTR spectrum up to the 7th order of resonance.

The cut-off wave-guide with diameter of  $\varnothing = 10$  mm (cutting out the frequencies  $\nu < 17.6$  GHz) we managed to isolate a single quasi-monochromatic line for  $k=7$  shown in figure 6. The spectral line width ( $\Delta\nu = 0.75 \pm 0.04$  GHz) is closed to the interferometer resolution. It means that the effective number of bunches radiating coherently is certainly larger than the value of  $N_{b\text{eff}} > \nu / \Delta\nu = 25$ .

In the case of the CDR investigation, the target geometry was changed as presented in figure 2 (see insertion). To compare the CTR and CDR spectra, the microtron was operated in the same regime. For CDR investigation we used the BCW with diameter of  $\varnothing = 15$  mm ( $\nu > 11.8$  GHz). The  $\theta$ -scan of the radiation intensity is shown in figure 7. In contrast to the CTR or CDR from a slit [25] the  $\theta$ -scan contains a single maximum along the specular reflection direction because here CDR is generated by a target edge only (see figure 7). The interferogram measured for  $\theta = \theta_m / 2$ , where  $\theta_m$  is the angle of specular reflection, is presented in the insertion in figure 8.

Table 3. Comparison of the resonance frequencies

$k$	$\nu_k$ (GHz)	$\nu_p$ (GHz)
4	10.5	10.5
5	13.2	13.3
6	15.8	15.8
7	18.4	18.5
8	21.0	-
9	23.6	-

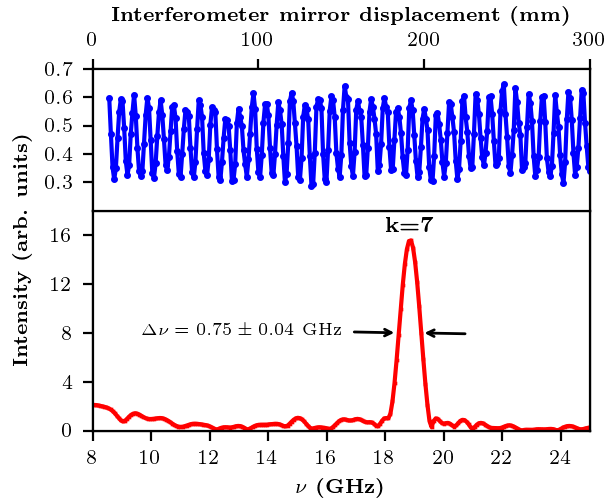


**Figure 6.** CTR spectrum (bottom) reconstructed from the interferogram (top) measured using the BCW with diameter of  $\varnothing = 10$  mm.

The CDR interferogram has a periodic amplitude modulation with period of  $\Lambda/2$  as well as CTR. The spectrum reconstructed from the measured interferogram is shown in figure 8. Thus, the CDR spectrum is analogous to the CTR spectrum in frequency range limited by the BCW. The difference might appear due to the fact that the CDR photon yield and the spectral content depend on the impact-parameter. For large impact-parameter  $h > \gamma\lambda$  the high frequency part of a CDR spectrum is suppressed. However, in our case this effect is small because  $h = 15\text{mm} \ll \gamma\lambda$ .

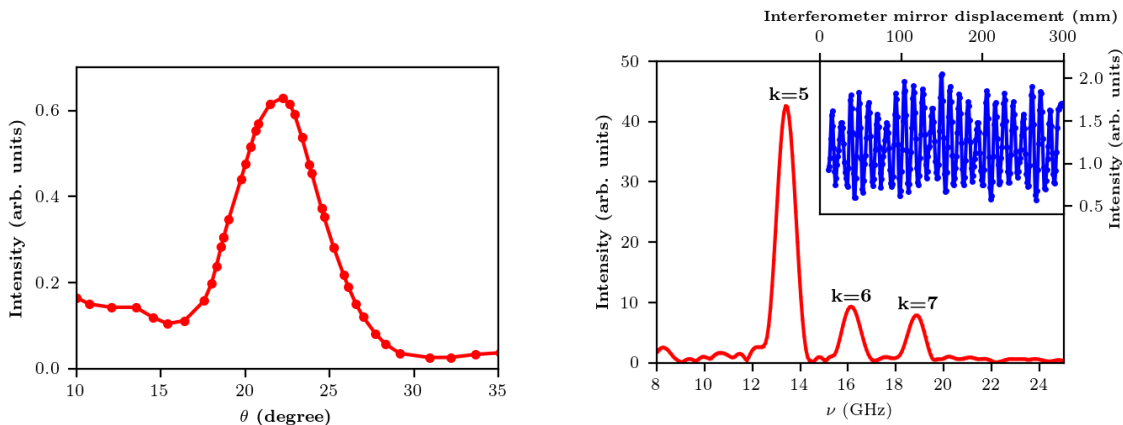


**Figure 7.**  $\theta$  - scan for the CDR geometry.

**Figure 8.** Spectrum reconstructed from the measured CDR interferogram shown in insertion.

#### 4. Discussion

We have demonstrated a possibility to generate monochromatic radiation using a prebunched electron beam. We managed to select or even isolate spectral lines with high diffraction orders using cut-off wave-guides. Another possibility to achieve high monochromaticity  $\Delta\nu_k / \nu_k \sim 10^{-2}$  even for a small number of bunches ( $N_b < 10$ ) is the use of a grating with period  $d \sim \lambda$  instead of a traditional flat CTR target. Choosing the grating period

and its tilt angle  $\theta$  it is possible to decrease the line bandwidth  $\Delta\nu_k$  significantly. As we demonstrated in [26] the resulting radiation, so-called “grating transition radiation” (GTR), becomes monochromatic due to constructive interference of electromagnetic fields generated on each grating element. The GTR monochromaticity is determined by the transverse radius of the relativistic particle Coulomb field  $\gamma\lambda$ , the number of effective periods, and the diffraction order,  $k$ :

$$\Delta\nu_k / \nu_k \sim \frac{1}{k} \frac{d \sin \theta}{\gamma\lambda}$$

CTR from a train and GTR have the same origin mechanism but their joint effect may lead to effective isolation of a spectral line of interest and to reject the rest due to the difference between periodicity of spectral lines for CTR from a train and GTR from a single bunch.

Figure 1 illustrates that the envelope of the spectrum “carries” information about the average bunch length,  $\sigma_z$ , in a train. A precise measurement of this envelope can be made with interferometer resolution  $\Delta\nu_{\text{exp}}$  much higher than  $\Delta\nu_k$  in order to avoid large distortion of the spectral line shape. The interferometer detector has to cover a wide frequency range around characteristic frequency  $\nu_0 = c/\sigma_z$ .

## Acknowledgments

This work was supported by the Ministry of Education and Science of the Russian Federation (program “Science,” basic part, No 3.8427.2017/8.9), by the Competitiveness enhancement program of Tomsk Polytechnic University, and by the Leverhulme Trust Foundation (International Science Network, project no. IN-2015-012).

## References

- [1] D. Mihalcea, C.L. Bohn, U. Happek, and P. Piot, *Longitudinal electron bunch diagnostics using coherent transition radiation*, *Phys. Rev.* **ST-AB 9**, 082801 (2006).
- [2] T. Takahashi, T. Matsuyama, K. Kobayashi, Y. Fujita, Y. Shibata, K. Ishi, and M. Ikezawa, *Utilization of coherent transition radiation from a linear accelerator as a source of millimeter-wave spectroscopy*, *Rev. Sci. Instrum.* **69**, 3770 (1998).
- [3] S. Casalbuoni, B. Schmidt, P. Schmser, V. Arsov, and S. Wesch, *Ultrabroadband terahertz source and beamline based on coherent transition radiation*, *Phys. Rev.* **ST-AB 12**, 030705 (2009).
- [4] V.L. Ginzburg and V.N. Tsytovich, *Transition Radiation and Transition Scattering*, Adam Hilger, Bristol, New York, 1990
- [5] B.M. Bolotovskiy, E.A. Galst'yan, *Diffraction and diffraction radiation*, *Physics - Uspekhi* **43** (8) 755 - 775 (2000)
- [6] J.D. Jackson, *Classical Electrodynamics, 3rd ed.* J. Willey&Sons, New-York, 1998.
- [7] R.A. Marsh, A.S. Kesar, and R.J. Temkin, *Absolute scale power measurements of frequency-locked coherent transition radiation*, *Phys. Rev.* **ST-AB 10**, 082801 (2007).



- [8] Y. Shibata, S. Sasaki, K. Ishi, *Coherent radiation from bunched electrons and prebunched FEL in the millimeter wavelength region*, *NIM A* **483** 440 (2002)
- [9] Y. Shibata, T. Takahashi, K. Ishi et al., *Observation of interference between coherent synchrotron radiation from periodic bunches*, *Phys. Rev. A* **44** R3445 (1991)
- [10] A. Gover, *Superradiant and stimulated-superradiant emission in prebunched electron-beam radiators. I. Formulation*, *Phys. Rev. ST-AB* **8**, 030701 (2005)
- [11] B.E. Billinghamurst, J.C. Bergstrom, L. Dallin et al., *Observation of superradiant synchrotron radiation in the terahertz region*, *Phys. Rev. ST-AB* **16** 060702 (2013)
- [12] S.F. Korbly, A.S. Kesar, J.R. Sirigiri et al., *Observation of Frequency-Locked Coherent Terahertz Smith-Purcell Radiation*, *Phys. Rev. Letters* **94** 054803 (2005)
- [13] G.A. Naumenkoa, A.P. Potylitsyn, P.V. Karataev, M.A. Shipulya, and V.V. Bleko, *Spectrum of coherent transition radiation generated by a modulated electron beam*, *JETP Letters* **106** 2 (2017)
- [14] Zhigang He, Yantang Xu, Wciwei Li, Oika Jia, *The PyZgoubi framework and the simulation of dynamic aperture in fixed-field alternating-gradient accelerators*, *NIM A* **775** 77 (2015)
- [15] Y.E. Sun, P. Piot, A. Johnson et al., *Tunable Subpicosecond Electron-Bunch-Train Generation Using a Transverse-To-Longitudinal Phase-Space Exchange Technique*, *Phys. Rev. Letters* **105** 234801 (2010)
- [16] P. Piot, Y.E. Sun, T.J. Maxwell, J. Ruan, A.H. Lumpkin, M.M. Rihaoui, and R. Thurman-Keup, *Observation of Coherently-Enhanced Tunable Narrow-Band Terahertz Transition Radiation from a Relativistic Sub-Picosecond Electron Bunch Train*, *Appl. Phys. Lett.* **98**, 261501 (2011).
- [17] A. P. Potylitsyn, *Transition radiation and diffraction radiation. Similarities and differences*, *Nucl. Instrum. Methods Phys. Res. B* **145**, 169 (1998).
- [18] N. F. Shulga and S. N. Dobrovolsky, *About transition radiation by relativistic electrons in a thin target in the millimeter range of waves*, *Phys. Lett. A* **259**, 291 (1999).
- [19] L. Frolich, *Bunch Length Measurements Using a Martin-Puplett Interferometer at the VUV-FEL*, DESY-Thesis 2005-011.
- [20] A. N. Aleinik, A. S. Aryshev, B. N. Kalinin, G. A. Naumenko, A. P. Potylitsyn, G. A. Saruev, A. F. Sharafutdinov, O. Yu. Malakhovskii, and E. A. Monastirev, *Coherent diffraction radiation of a 6-MeV microtron electron beam*, *JETP Lett.* **76**, 337 (2002).
- [21] D. H. Martin and E. Puplett, *Polarised interferometric spectrometry for the millimetre and submillimetre spectrum*, *Infrared Phys.* **10**, 105 (1970).
- [22] D. K. Lambert and P. L. Richards, *Martin-Puplett interferometer: an analysis*, *Appl. Opt.* **17**, 1595 (1978).
- [23] V. M. da Costa and L. B. Coleman, *Theory of a double polarization modulated Martin-Puplett interferometer*, *Appl. Spectrosc.* **44**, 1301 (1990).
- [24] A.N. Aleinik, O.V. Chefonov, B.N. Kalinin, G.A. Naumenko, A.P. Potylitsyn, G.A. Saruev, A.F. Sharafutdinov, W. Wagner. *Low-energy electron-beam diagnostics based on the optical transition radiation*. *NIM B* **201** (2003) 34-43

- [25] G.A. Naumenko, A.N. Aleinik, A.S. Aryshev, B.N. Kalinin, A.P. Potylitsyn, G.A. Saruev, A.F. Sharafutdinov. *Coherent transition and diffraction radiation from a bunched 6.1MeV electron beam*. *NIM B* **227** (2005) 70-77
- [26] A. P. Potylitsyn, G. A. Naumenkoa, L. G. Sukhikh, A. Aryshev, M. Shevelev, N. Terunuma, and J. Urakawa. *Observation of Subterahertz Monochromatic Transition Radiation from a Grating*. *JETP Letters* **104** 11 (2016) 806–810.